

DOI: 10.1002/adma.200702126

# Mass-Productions of Vertically Aligned Extremely Long Metallic Micro/Nanowires Using Fiber Drawing Nanomanufacturing\*\*

By Xuejun Zhang, Zeyu Ma, Zhong-Yong Yuan, and Ming Su\*

One dimensional microwires and nanowires are unique emerging advanced materials that could be used in many areas including microelectronics, composite materials, biological sensing and separation, etc.<sup>[1,2]</sup> In many cases the micro/nanowires should be properly aligned in order to achieve desired functionalities.<sup>[3]</sup> However, fabricating such an array of ordered micro/nanowires at high production yield is a great challenge to most of current methods, where a cheap material should be processed in an economic way. Chemical or physical vapor deposition often produces tangled nanowires that need to be further processed for desired functions, and the simultaneous controls over their diameter, length, position and orientation have not been achieved. Electrical field manipulation and hydrodynamic flows do not offer sufficient controls to place nanowires at desired locations with high reliability,<sup>[4]</sup> and the direct manipulation over single nanowire has an extremely low yield.<sup>[5]</sup> Meanwhile, although surface bounded micro/nanowires can be useful in making electronic circuits, there are increasing needs to make vertically aligned micro/nanowires for specialized engineering applications such as solar energy conversions.

Ultrafine wires have been made in insulating porous matrices of alumina and silica, but the wires from the methods are unfortunately tangled. Anodized aluminum oxide (AAO) with ordered nanochannels can be used as template to make

nanowire arrays using electrochemical or vapor deposition.<sup>[6]</sup> But AAO is not ideal for applications where a large array of nanostructures is needed, because AAO template is fragile, covers a small area, and is hard to be mass-produced, handled and integrated. On the other hand, although lithographic techniques can provide great controls over the position and orientation of structures, the sizes of structures cannot be reduced at a reasonable cost. Photolithography and micro-machining only make microstructures.<sup>[7]</sup> Focused ion and electron beam lithographies are too slow and expensive to make structures that cover large areas.<sup>[8]</sup> Soft lithographic methods though versatile, still do not reach the level needed (yield, resolution and controllability) for manufacturing.<sup>[9]</sup> Most importantly, the lithographic methods and synthetic methods including AAO-template produce nanowires with limited length (or height), which brings urgent requirement for manipulation and connection. Actually, an ideal method should be able to produce micro- or nanowire arrays at high yields over large areas.

We propose a novel method for the mass-production of aligned micro- or nanowires by drawing glass tubes that contain appropriate filling materials in powder or rod form. Previously the fiber-drawing methods have been used to make glass nanochannel and nanocone arrays.<sup>[10,11]</sup> Our method combines fiber drawing method with advanced filling materials, thus providing not only desired functionality, but also excellent controls over the aspect ratio, diameter, length and interwire spacing of micro/nanowires. In addition, although this method could be applied to any solid materials as long as a matching glass could be found, the large-scale manufacturing nature of the fiber drawing requires that the cost of the filling material should be comparable to that of glass in order to maximize its manufacturability. Such consideration makes it necessary to find some cheap and easy-to-get materials that could be processed reliably. Therefore, another goal of our work is to identify economic materials for large-scale fabrications of micro/nanowire arrays.

In fiber drawing nanomanufacturing, pouring powders or inserting a rod into a glass tube makes a preform for fiber drawing (Fig. 1). The fibers from the first drawing process are cut into short pieces of equal length, which are stacked together to form a hexagonal bundle for the next drawing cycle. By repeating the draw-cut-stack process for several times, the outer and the inner diameters, and the thickness of the glass tube will decrease from centimeters to hundreds nanometers.

[\*] Prof. M. Su, X. Zhang, Z. Ma  
NanoScience Technology Center, Department of Mechanical,  
Materials, and Aerospace Engineering, University of Central Florida  
Orlando, Florida 32826 (USA)  
E-mail: mingsu@mail.ucf.edu

X. Zhang, Dr. Z.-Y. Yuan  
College of Chemistry, Nankai University  
Tianjin, 300071 (P. R. China)

[\*\*] X. Z. and Z. M. contributed equally to this work. We appreciate the guidance from Dr. D'Urso at Oak Ridge National Laboratory over the past years, and thank Mr. Modlin at Advantak Engineering for instrumentation assistance. The project is supported by a New Investigator Research Award from the James and Esther King Biomedical Program of the Florida Department of Health, a Starter G grant from Petroleum Research Fund of American Chemical Society, a grant from Florida Space Grant Consortium and an In-house research grant from University of Central Florida (UCF). Most of characterizations were done at the Materials Characterization Facility at UCF. The SIMS images were collected at the NUANCE facility at Northwestern University. X. Zhang is a visiting student from Nankai University and is financially supported by UCF during the work.

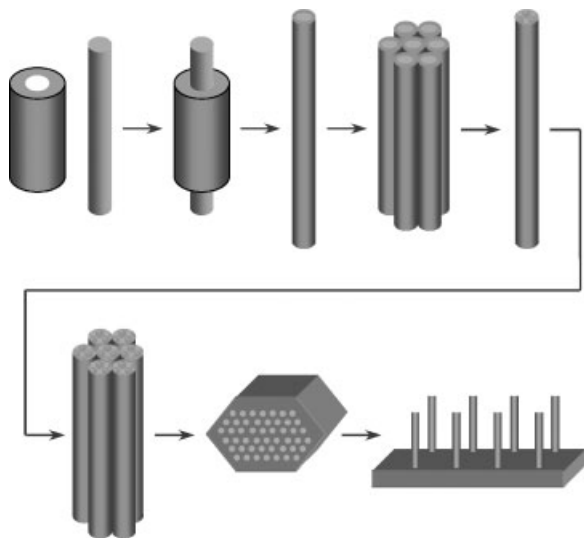


**Figure 1.** Scheme of making aligned micro/nanowires using fiber-drawing nanomanufacturing.

Meanwhile the ordered arrangement of fibers is preserved. After the last drawing, the fibers are stacked and annealed below the softening temperature of the glass to make a solid rod. Finally, the rod is cut perpendicular to its axis to make plates that have ordered array of micro/nanowires of the filling materials. This process especially the first drawing is analogous to powder metallurgy process. After making encapsulated nanowires, the glass could be removed easily by dipping fibers into hydrogen fluoride, leaving extremely long nanowires over meters. Although the material-containing glass fibers from the last drawing are intentionally chopped to short pieces for packing, the same drawing method has been routinely used to make optical fibers in telecommunications. A vacuum pump is connected to the glass tube, and the drawing is done in vacuum to avoid the possible oxidation of the filling materials and to make an intimate contact between the glass and the filling materials.

This method has a reasonable size reduction mechanism and high yield. From geometric consideration, the ratio of the size reduction depends on the diameters of the starting preform or rod and the obtained fibers, and thermophysical properties of glass and material at the drawing temperature. The glass tubes used in our experiment has 7.6 mm outer diameter, 1.6 mm inner diameter and 3 mm wall thickness. The diameters of glass-material composite fibers that can be reliably drawn and cut usually fall between 250 and 600  $\mu\text{m}$ . We have chosen  $380 \mu\text{m} \pm 20 \mu\text{m}$  as the target diameter, because the glass fibers with such diameter are relatively strong, easy to handle and pack, and has reasonable size scaling ratio for the first and second draws. Providing the thermophysical properties of the glass and the material are constant, the designed diameter of microwires can be derived from simple calculation. Starting from a core diameter of 1.6 mm, the diameters of the core material become  $80 \mu\text{m}$  after the first draw with a scaling ratio of 20. The fiber pieces are packed inside a glass tube that has an

inner diameter of 15.6 mm and an outer diameter of 17.7 mm. The as-drawn fibers have the diameters at  $2 \mu\text{m}$  and  $50 \text{ nm}$  after the second and third draw cycle with an identical scaling ratio of 40. The same scaling ratio will be applied to wall thickness, namely the spacing between adjacent two microwires. Assuming there is no material loss during each drawing with the scaling ratio of 20, 40 and 40, we have estimated the productivity of fiber drawing nanomanufacturing. Starting from a 1.5 m long and 1.6 mm inner diameter preform, we will obtain  $9 \times 10^8$  nanowires (1.5 m in length and  $50 \text{ nm}$  in diameter) after three consecutive draw-cut-stack cycles. At a typical draw speed of  $2 \text{ m s}^{-1}$ , each draw step (first, second, and third) will take 4.4 min, 20 min, and 20 min. Eventually, the glass-material rod could be cut into 750 plates of 2 mm thick and 7.8 mm in diameter with a total length of all nanowires over  $1.35 \times 10^9 \text{ m}$ . The draw speed could be increased up to  $20 \text{ m s}^{-1}$  on industrial scale draw towers, which take large preform and have long distance between the outlet of furnace and the pulling device, thus providing sufficient time to cool down the fiber even at the large draw speed.

We have made a metallic microwire array by inserting a 1 mm diameter copper-phosphor alloy rod or powders (92.75% Cu and 7.25% P) into a Pyrex glass tube to form a preform for the fiber drawing. The melting point of the alloy ( $725^\circ\text{C}$ ) is close to the drawing temperature of the glass ( $850^\circ\text{C}$ ). The morphologies and compositions of the microwires and arrays are studied by a JEOL 6400 field emission scanning electron microscope (SEM). Figure 2A is the SEM image of a broken glass fiber containing an alloy microwire obtained during the first draw. The microwire forms good contact with the glass shell, and bent off the center, indicating its good ductility. The bundle of fiber pieces is annealed, and the glass-microwire composite is cut perpendicular to its axis into thin plates. In the next, the plates are polished using grits of different grade. Figure 2B is the SEM image taken at the cross section of the plate, where the microwires form a hexagonal array. The white

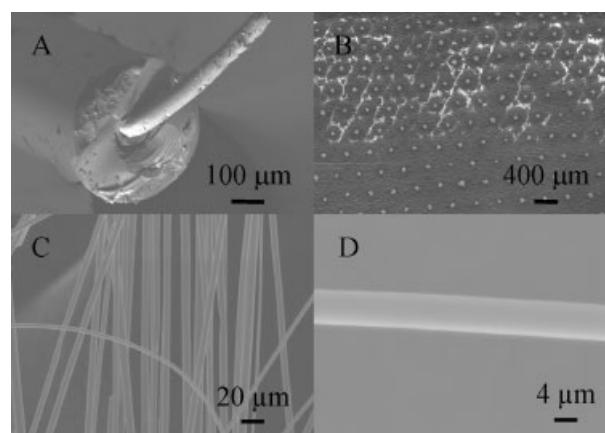


**Figure 2.** SEM images of glass encapsulated copper-phosphor microwire (A) and the large array of the copper-phosphor microwires (B) after the first draw cycle. Copper-phosphor microwires (C and D) made in the second drawing, where the glass coating is removed before imaging.

lines around each dot are the result of charging on the insulating glass, as the plate was not covered with a conductive film prior to imaging. The size of the metal wires can be reduced to several micrometers by repeating the draw-cut-stack cycle for a second time. In order to confirm the formation of continuous microwires, the glass coatings around some microwires are removed by immersing the fibers into a 10% aqueous hydrogen fluoride solution. Figure 2C and 2D show the SEM images of the straight copper-phosphor microwires, where the diameters are uniform over a length of several centimeters.

The fiber pieces of equal length are encircled in a glass tube to pack densely, followed by annealing at 750 °C to form a glass-microwire composite rod. We have used secondary ion mass spectrometer (SIMS) to obtain element distributions of phosphor and copper on the cross section of microwire-glass rod. Figure 3A and 3B are the SIMS images collected using the characteristic signals of copper and phosphor, respectively. The coincidence of copper and phosphor signals in the images suggests the uniform distribution of the elements on the cross-sections of microwires. The diameters of copper-phosphor wires become smaller after the third drawing. Figure 3C and 3D show the SEM images of the copper-phosphor nanowires after removed the glass coating by immersing the fiber in the 10% hydrogen fluoride solution. In the case where non-coated nanowires are needed, we may evaporate a layer of appropriate material to one end of the bundle, thus the ordered arrays can be preserved even after removing the glass shells. X-ray diffraction (XRD) analysis has been done on the micro/nanowire glass plates using a Rigaku diffractometer with Cu-K $\alpha$  line radiation. Figure 3E indicates that the intensity of diffraction peak around 44.5° has changed compared to original powder and JCPDS diffraction data. The XRD curves from the top to the bottom are those collected from the starting powder, the plates obtained after the first, second and the third draw-cut-stack cycles, respectively. A slight shift of diffraction peak to high angle has been observed, which may be due to the evaporation of phosphor at high temperature. In addition, some peaks do not appear when the diameters decrease, which could be induced by the decrease of the relative amount of copper phosphate after being packed inside the glass tubes. Assuming there is no material loss, the volume ratios of the alloy to glass are 5.75%, 4.01% and 2.84% after the first, second and third drawing. The actual decreases of the alloy to glass ratios would

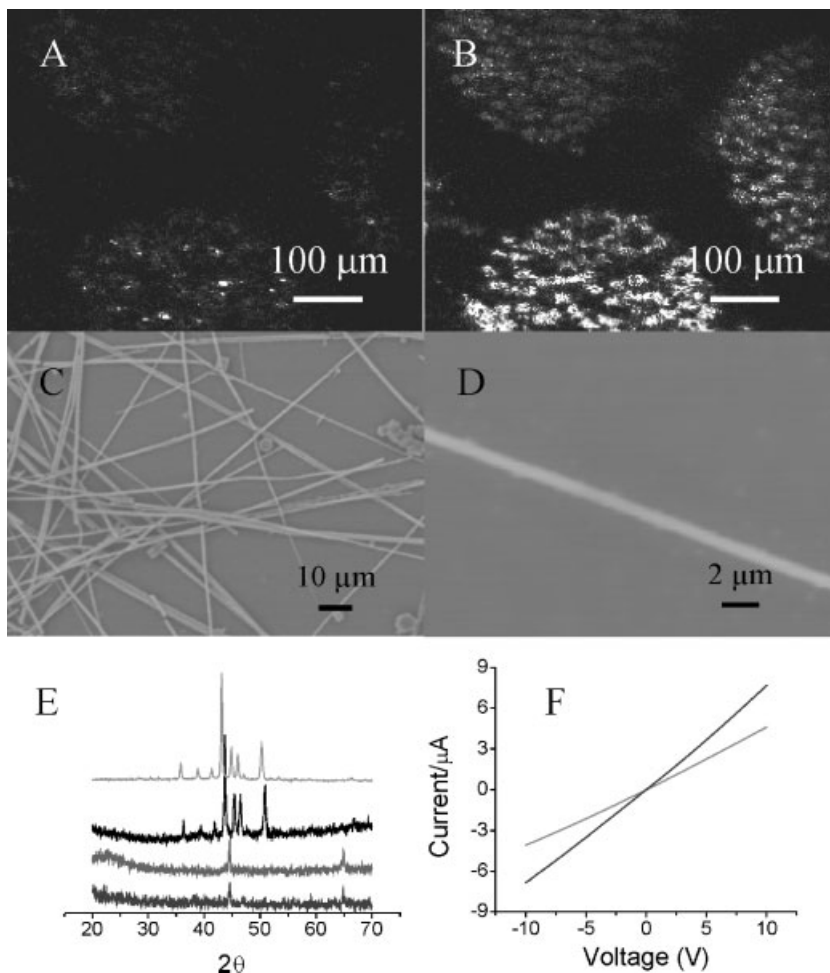


**Figure 3.** The distributions of phosphor (A) and copper (B) on a flat plate after the second draw-cut-stack cycle obtained using SIMS; SEM images of copper-phosphor nanowires obtained in the third draw cycle after removing glass coating (C and D); XRD curves of the copper-phosphor powder, and those obtained after the first, second and third draws (from top to bottom) (E); the current-voltage relation measured across an array of microwires (F).

be larger than these values due to the alloy loss. The electrical properties of microwires across a polished glass plate are measured by using a Keithley 2400 sourcemeter. The microwire array shows high conductivity, and the current saturates rapidly even at a low voltage. In order to measure the current *versus* voltage relation of the bundled microwires, we have connected two resistors in series to an array of microwires. The linear curves suggest there is no oxidation of the copper-phosphor alloy wires in vacuum in the high temperature drawing process (Figure 3F).

The compositions of micro/nanowires made by fiber drawing nanomanufacturing have been studied using energy dispersive X-ray analysis (EDX), operating at the acceleration voltage of 15 kV. The interaction volume of the electron beam with copper-phosphor alloy can be derived from the equation:<sup>[12]</sup>

$$x(\mu\text{m}) = \frac{0.1 \cdot E^{1.5}}{\rho} \quad (1)$$

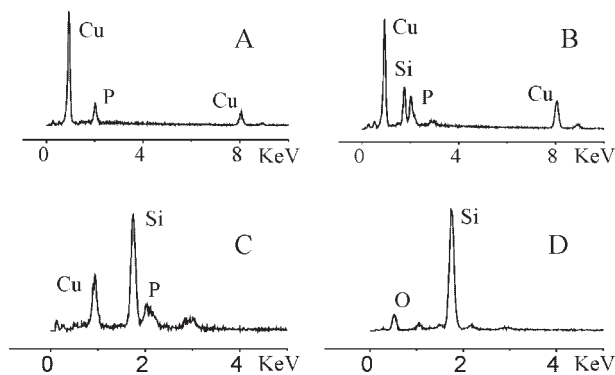


**Figure 4.** EDX spectra of copper-phosphor micro/nanowire after the first (A), second (B) and third (C) draw cycle, and the comparison to that on a near-by glass region (D).

where  $E$  is the acceleration voltage in  $kV$ ,  $\rho$  is the density of the material in  $g\ cm^{-3}$ . Taking the density of copper ( $8.9\ g\ cm^{-3}$ ), the electron beam penetrates the alloy with an approximate depth of  $650\ nm$ . At such a depth, the electron beam cannot pass through microwires from sidewalls to give the overall compositions, but only the surface concentrations on the sidewalls. EDX spectra collected on the sidewalls of the fibers obtained in the first, second and third draw cycles show the existence of copper (Fig. 4A and C), and the EDX spectrum from the glass region around a microwire shows no copper peak (Fig. 4D), excluding the possibility of the reaction between copper phosphor and the glass. Compared to the starting powder, the compositions of microwires change slightly. The amount of copper relative to phosphor has decreased from 92.75% to 85.6% after the first draw (Fig. 4A). After the second and the third draw cycles, the relative amounts of copper change to 89.9% and 78.4% as shown in Figure 4B and 4C. Considering that phosphor has a lower melting point of  $44.1\ ^\circ C$  and higher vapor pressure than that of copper at the same temperature, phosphor will be preferentially evaporated from the melt of copper-phosphor during the high temperature drawing in vacuum. After reaching thermodynamic equilibrium in furnace, the concentration of phosphor at the outer surface of a melted microwire will increase. The high concentration of phosphor is preserved even after the fiber is pulled out of the furnace due to the temperature decrease. In addition, the surface enrichment of phosphor is supported by the fact that the surface

color of the microwire changes to red, which is characteristic for phosphor.

In the fiber drawing experiments, the scaling ratio of diameter reduction does not exactly follow the designed value based only on the geometric considerations. Starting from the  $1.5\ mm$  inner diameter glass tube filled with the copper-phosphor powder, the diameters of the obtained wires will decrease to  $66\ \mu m$ ,  $7.2\ \mu m$  and  $500\ nm$  after the first, second and third draw cycle, respectively. Providing that the total scaling ratio is the product of the scaling ratios of individual steps, thereby, the actual total scaling ratio will be  $2914.6$  ( $= 22 \times 9.2 \times 14.4$ ) obtained from SEM images, which is ten times less than the designed total scaling ratio of  $32000$  ( $= 20 \times 40 \times 40$ ). The variation leads to the difference in the designed diameter ( $\sim 50\ nm$ ) and the actual diameter ( $\approx 500\ nm$ ) in a cumulative way. We have not etched the glass in the final glass rod completely, because that would need significant amount of etchant. But more than ten samples have been made from the same rod, and all of them show significant amount of continuous nanowires in SEM images. Such variations are believed to be the results of composition changes of microwires during fiber drawing. The surface

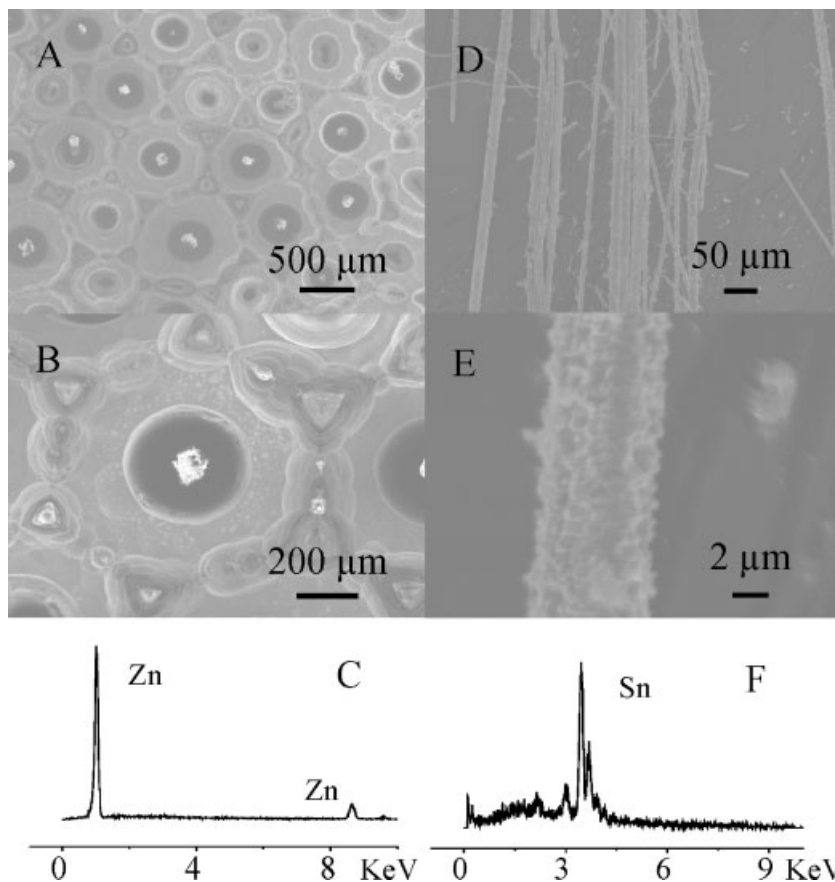


**Figure 5.** SEM images of zinc microwires embedded in glass matrices (A and B) and the according EDX spectrum (C); SEM images of tin microwires after removing the glass coating (D and E) and the according EDX spectrum (F).

enrichment of phosphor increases the relative amount of phosphor, which changes the mechanical and thermophysical properties of microwires after each draw. It has been found the higher the phosphor content, the less ductile the alloy.<sup>[13]</sup> For a crystalline material such as the copper phosphate alloy at eutectic composition, the melting range is very narrow. A slight composition change off the eutectic composition could lead to an increase in the melting point, which could lead to the change in coefficient of thermal expansion of the alloy. The formation of a microwire with phosphor-rich shell and copper-rich core increases the resistance for the glass tube to shrink, thus the diameter of microwires will increase. Actually, the diameter of microwire could also become smaller in other situations. When powders of an inorganic material (sodium chloride) are filled inside a glass tube with the same composition, the diameter of the microwire is 2–3 times smaller than the designed value (figure not shown).

The similar approach can be used to make micro/nanowires of other materials as long as the matching filling material and glass material can be identified. For instance, we have used the method to make one-dimensional structures of zinc and tin using their powders. Bulk zinc and tin have melting points at 420 °C and 232 °C. At the drawing temperature 850 °C, both materials are in liquid state and have high vapor pressures. Zinc powders have been drawn into microwires that have been stacked to form a metal-glass composite rod as shown in the cross-section SEM image (Fig. 5A). The interstitial space (dark ring around the wire) is induced by the partial annealing of glass, or the difference in coefficients of thermal expansion of the glass and zinc (Fig. 5B). EDX spectrum confirms that the microwire inside the circular glass ring is made of zinc (Fig. 5C). In the case of tin, some materials condense on the inner wall of the tube close to the vacuum inlet due to the high vapor pressure of tin at 850 °C. Some air gaps form along microwires, thus making segments of several centimeters long. The discontinuity could be the result of the poor wettability of the melted tin to glass surface.<sup>[14]</sup> After the second draw, the glass coating around tin microwires are removed, leaving straight microwires of tin (Fig. 5D). High-resolution SEM image (Fig. 5E) indicates that the surface of tin microwire is rough and has many nanoscale protrusions, which could be induced by the tendency of melted tin to reduce its energy inside the glass. The EDX spectrum collected on the microwire confirms the existence of tin (Fig. 5F).

From these trial-and-try studies, we have derived several criteria for the success of fiber drawing in making micro- or nanowires: (1) the softening temperature of the glass is

between the melting temperature and the boiling temperatures of the filling material; (2) the coefficients of thermal expansion of the glass and the filling material at the drawing temperature are close to each other, or the filling material is in liquid; (3) there is no chemical reaction between the glass and the material at the drawing temperature; (4) the molten material should have a certain wettability to the glass surface; (5) the materials should not have high vapor pressure at high temperature. Although these criteria seem rigorous, many choices are available with respect to glass composition and working conditions, making the method a general strategy. In contrast to the Tylor wire process that has been practiced to make glass encapsulated microwires for several decades,<sup>[15]</sup> our method has the appropriate size reduction mechanism to draw fiber with nanometer diameter, and assemble such micro- or nanowires into ordered arrays. In principle, by using glass tube or other tubular materials with appropriate thermo-physical, chemical and surface properties, we should be able to make vertically aligned micro/nanowires of any metallic materials over a large area at high yield, controllability and manufacturability.

Received: August 22, 2007

Revised: October 19, 2007

Published online: March 7, 2008

- [1] S. Iijima, *Nature* **1991**, 354, 56.
- [2] J. Kong, N. R. Franklin, C. W. Zhou, M. G. Chapline, S. Peng, K. J. Cho, H. J. Dai, *Science* **2000**, 287, 622.
- [3] K. D. Hermanson, S. O. Lumsdon, J. P. Williams, E. W. Kaler, O. D. Velev, *Science* **2001**, 294, 1082.
- [4] Y. Huang, X. Duan, Q. Wei, C. M. Lieber, *Science* **2001**, 26, 630.
- [5] T. Hertel, R. Martel, Ph. Avouris, *J. Phys. Chem. B* **1998**, 102, 910.
- [6] K. Nielsch, F. Muller, A.-P. Li, U. Gosele, *Adv. Mater.* **2000**, 12, 582.
- [7] L. R. Harriott, *Proc. IEEE* **2001**, 89, 366.
- [8] J.-F. Li, S. Tanaka, T. Umeki, S. Sugimoto, M. Esashi, R. Watanabe, *Sens. Actuators A* **2003**, 108, 97.
- [9] Y. Xia, G. M. Whitesides, *Angew. Chem. Int. Ed. Eng.* **1998**, 37, 550.
- [10] R. J. Tonucci, B. L. Justus, A. J. Campillo, C. E. Ford, *Science* **1992**, 258, 783.
- [11] B. R. D'Urso, J. T. Simpson, M. Kalyanaraman, *J. Micromech. Microeng.* **2007**, 17, 717.
- [12] P. J. Potts, in *A Hand Book of Silicate Rock Analysis*, Chapman and Hall, NY **1987**, p. 336.
- [13] R. F. Sim, J. A. Wilingham, *FWP J.* **1987**, July 33.
- [14] F. Delannay, L. Froyen, A. Deruyttere, *J. Mater. Sci.* **1987**, 22, 1.
- [15] I. W. Donald, *J. Mater. Sci.* **1987**, 22, 2661–2679.